Artificial Life and Robotics
https://doi.org/10.1007/s10015-020-00592-9

INVITED ARTICLE

Brain–machine interfaces using functional near-infrared spectroscopy: a review

Keum-Shik Hong[1] · Usman Ghafoor[1] · M. Jawad Khan[2]

Received: 2 September 2019 / Accepted: 14 February 2020

Abstract
Functional near-infrared spectroscopy (fNIRS) is a noninvasive method for acquiring hemodynamic signals from the brain with advantages of portability, affordability, low susceptibility to noise, and moderate temporal resolution that serves as a plausible solution to real-time imaging. fNIRS is an emerging brain imaging technique that measures brain activity by means of near-infrared light of 600–1000 nm wavelengths. Recently, there has been a surge of studies with fNIRS for the acquisition, decoding, and regulation of hemodynamic signals to investigate their behavioral consequences for the implementation of brain–machine interfaces (BMI). In this review, first, the existing methods of fNIRS signal processing for decoding brain commands for BMI purposes are reviewed. Second, recent developments, applications, and challenges faced by fNIRS-based BMIs are outlined. Third, current trends in fNIRS in combination with other imaging modalities are summarized. Finally, we propose a feedback control concept for the human brain, in which fNIRS, electroencephalography, and functional magnetic resonance imaging are considered sensors and stimulation techniques are considered actuators in brain therapy.

Keywords Functional near-infrared spectroscopy · Brain–machine interface · Classification · Stimulation · Neuromodulation

1 Introduction

A brain–machine interface (BMI) or brain–computer interface (BCI) is a software and hardware communication system that can be used to bridge the gap between thoughts and actions, allowing people with physical disabilities (PWPD) to control external devices or communicate with the real world. BMI systems are designed to benefit PWPD by facilitating increased independence in functional areas such as communication, mobility, and access to computers and electronic aids for day-to-day living. These systems rely on the control signals generated from the brain and are executed without the involvement of peripheral nerves and muscles [1]. In the last two decades, several studies have emerged showing great potential in developing BMI applications for a variety of patients who cannot control their muscle movements voluntarily or for PWPD who suffer from illnesses including locked-in syndrome, amyotrophic lateral sclerosis (ALS), primary lateral sclerosis, hemi- and tetra-plegia, Duchenne muscular dystrophy, traumatic brain injury, stroke, cerebral palsy, multiple sclerosis, Parkinson's disease, spinal cord injury, progressive supranuclear palsy, spinocerebellar ataxia, and spinal muscular atrophy [2, 3]. The development of BMI applications is essential in the current era due to an increase in the population of elderly people (age > 60) in society. A recent survey conducted by the United Nations has shown that the population of seniors is expected to grow by approximately nine billion by the year 2050 [4]. A graph of the yearly trend of the population of elderly individuals is shown in Fig. 1. Since diseases such as Parkinson's disease and locked-in syndrome can be more commonly found in elderly people, extensive developments have been made by researchers and scientists to improve

This work was presented in part as a plenary speech at the 22nd International Symposium on Artificial Life and Robotics, Beppu, Oita, January 19–21, 2017. The authors submitted the modified draft in response to the invitation.

✉ Keum-Shik Hong
kshong@pusan.ac.kr

1 School of Mechanical Engineering, Pusan National University, 2 Busandaehak-ro 63beon-gil, Geumjeong-gu, Busan 46241, Republic of Korea

2 School of Mechanical and Manufacturing Engineering, National University of Science and Technology, Islamabad 44000, Pakistan

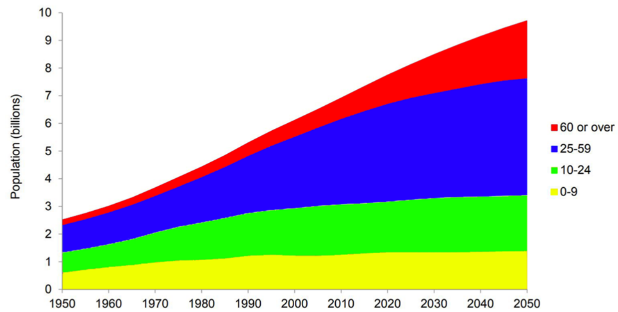

Fig. 1 Expected global population by the year 2050 [4]

BMI methods that can cope with potential issues raised by an aging society and serve as neurorehabilitation tools for individuals with severe motor impairment.

To establish communication between the brains of PWPD and computers, a basic BMI scheme comprises five steps: (1) signal acquisition; (2) preprocessing or signal enhancement; (3) feature extraction; (4) classification; and (5) the control interface [5]. Steps 2–5 are extensively discussed in the literature. Here, the primary focus is on the brain signal-acquisition stage, which is crucial in both invasive and noninvasive types of BMIs [6]. There are two types of brain signals detected using noninvasive brain imaging. The first type is neuronal signals that are directly acquired from the scalp as electric potentials using metal electrodes; the second type is known as hemodynamic signals that are generated as a result of oxygen exchange in the blood caused by neuronal firing. Electroencephalography (EEG) signals are electric potentials generated due to neuronal firing when some mental activity is performed, which can be used for BMI applications [7, 8]. On the other hand, functional near-infrared spectroscopy (fNIRS) and functional magnetic resonance imaging (fMRI) can be used for BMI applications that measure hemodynamic activity [9–11]. The increased blood flow due to activated neurons results in an increase and decrease of oxy- and deoxyhemoglobin, respectively, which can be observed using fNIRS.

Interestingly, in 1999, in parallel to the work of Chapin and Nicolelis on animals with invasive BMIs, Niels Birbaumer led the group at the University of Tubingen in Germany and posed their pioneered work that established a direct link between the brain and a computer in patients with locked-in syndrome [12, 13]. Birbaumer named this direct link BMI, which had been introduced in the literature two decades ago [14]. Using this noninvasive BMI, locked-in patients were able to write messages on the computer with brain signals (cortical potentials) measured through EEG. As an imaging modality for BMIs, EEG is commonly used for studies because it is low in cost, portable, and noninvasive [15–17]. It has a high temporal resolution that enables the detection of brain activity at millisecond resolution. Motor imagery (MI), steady-state visual evoked potentials (SSVEP), and P300 evoked potentials are commonly used brain signals for BMI development [18–22]. These brain-originated signals in the form of electric potentials have been applied to control BMI devices, such as wheelchairs and quadcopters [23–26].

In addition to EEG, another modality commonly used for BMIs is fNIRS, which utilizes light in the near-infrared range between 600 ~ 1000 nm to measure the hemodynamic changes in the form of oxygenated hemoglobin (ΔHbO) and deoxygenated hemoglobin (ΔHbR). The cerebral blood flow changes are measured from the cortical brain regions by detecting the absorption of near-infrared light and are associated with brain activity [27–33]. In comparison to fMRI, fNIRS provides spatially specific signals at high temporal resolution (~ 100 ms). It is portable, less expensive than fMRI, and considered safe to use. fNIRS employs multiple pairs of illuminators and detectors operating at two or more distinct wavelengths. Participants can be scanned under normal conditions, which make fNIRS a more viable option for implementing BMIs. Several previous studies have shown the feasibility of fNIRS for BMI applications and rehabilitation purposes [5, 6, 9, 34–36]. Since the focus of this review is on the fNIRS-based BMIs and challenges faced by this modality, we tried to circumvent other noninvasive techniques such as EEG and fMRI. However, studies on the combination of these modalities will be discussed in future prospects of BMI applications with imaging techniques. Such systems are called "Hybrids", which have been employed to obtain an increased number of control commands and improved classification accuracies for BMI applications [37–40].

BMI applications that incorporate both fNIRS and EEG can be categorized into three types: active, passive, and reactive. In an active-type BMI, to generate brain activity, various brain tasks are used: MI, motion intention, and mental tasks. During these tasks, the subjective brain activity is generated by the individual without any external stimuli. Reactive-type tasks use external stimuli to generate brain activity. In these paradigms, the stimulus can be given in the form of an audio, video, interrogative, or pain stimulus [41–43]. Generating a command is difficult in the case of active and reactive cases due to the limited ability of the user to consciously interact with multiple components simultaneously. Passive BMI or passive brain activity is an arbitrary activity that can be generated by the brain without voluntary control of a subject or user [15]. Characteristically, it is different from cognitive user state monitoring because an arbitrary activity generated without any objective control can be used. This is advantageous because several activities can be detected in parallel, further used the translation of commands in the development of a BMI system.

The present review aims to discuss progress in fNIRS-based BMIs. First, the procedures involved in the development of fNIRS-based BMIs will be discussed. Second, the brain activities that can be detected for BMIs and brain imaging using an fNIRS modality are discussed. Third, the challenges and problems that exist in noninvasive imaging-based BMIs are discussed. We will also discuss the role of fNIRS in the development of hybrid-type BMI systems for rehabilitation and brain therapy applications. Finally, we propose a closed-loop control scheme of the brain, where imaging modalities are considered sensors and stimulation methods are considered actuators to improve the brain therapy process for better generation of control commands.

2 Early advancements in fNIRS-based BMIs

In this section, we will summarize early advancements, from 2004 to 2011, made in the development of fNIRS-based BMI systems. This noninvasive imaging modality, introduced by Jobsis et al. in 1977, has been used for various applications [44]. Usually, PWPD prefer nonsurgical options in any clinical treatment, as their safety is of extreme priority; therefore, noninvasive BMIs are the default choice for clinical applications. The first fNIRS-based BMI was presented by Coyle et al. in 2004 [45]. In this preliminary study, the subjects were asked to perform a motor imagery task of squeezing a ball. The BMI achieved an overall 75% recognition of the subjects' imagined movements. After a gap of 2 years, in 2007, three more studies were published describing new fNIRS-based BMI concepts. A custom-built, simplified fNIRS device was designed to detect hemodynamic responses (HR) generated from mental imagery processes that could be used as a control (on–off) channel for a computer application [46]. Another potential application of fNIRS in the development of BMI applications was conducted by Sitaram et al. who successfully classified left-hand motor imagery from a right-hand MI task with an average accuracy of 73% for all healthy subjects using support vector machines (SVM) as a classifier [47]. The hidden Markov model (HMM) performed better as a classifier, with an average accuracy of 89%. A significant and pioneering study was conducted by Naito et al. to illustrate the concept of fNIRS-based BMIs for patients with amyotrophic lateral sclerosis in a totally locked-in state who were completely unable to move any part of the body [48]. Using quadratic discriminant analysis, the patients' intentions were correctly classified, with an accuracy of 80%. A total of four studies were conducted in 2008–2009. Although the expansion in the field was slow but represented a never-ending development towards optical measurement-based BMIs. On the one hand, in 2008, "Go-Stop" control using HR evoked from arithmetic calculations was demonstrated; on the other hand, in the same year, stable HRs that were opposite in nature and evoked from the frontal cortex of healthy subjects were reported, further suggesting the application of HR towards BMIs [49, 50]. In 2009, a group led by Tom Chau published two studies that demonstrated the feasibility of BMI development using the single-trial classification of fNIRS signals. A positive/negative emotional induction task was employed to distinguish HR features obtained from genetic algorithms from baseline levels in an offline analysis, with linear discriminant analysis (LDA) and SVM as a classifier, which ultimately provided accuracies up to 75% [51]. In their second study, the subject's preference towards one of their preferred drinks from two presented was decoded from the prefrontal cortex and was able to achieve an average accuracy of 80% with LDA [52]. In 2010, two more studies were published: in the first, HRs generated from mental arithmetic and music imagery tasks were classified with an average classification accuracy of 77.2% using HMM [53]. In the second study, a finger tapping task vs rest was classified using a multivariate pattern classification technique to enhance the viability of fNIRS-based BMIs and real-time applications [54].

In early developments, the steps followed to make the BMI system were the same as those alluded to in the Introduction section but varied in terms of classification techniques and task choice, i.e., either cognitive or motor imagery. A typical fNIRS-based BMI is shown in Fig. 2. This leads to a steering of the focus of our review towards the inclusion of later studies in terms of signal preprocessing methods, the activities involved in acquiring brain signals, and the classification techniques in the upcoming subsections. It was also noted that since there were fewer generated commands, there exists an information transfer gap, an inherent delay in the hemodynamic signal, and obtained accuracies that were not as good as in conventional, direct or invasive methods of controlling machines, or computers using the brain [55]. Therefore, promising techniques, such as the concept of hybrid BMIs (fNIRS-EEG, with the inclusion of physiological measurements) and reduction of delay

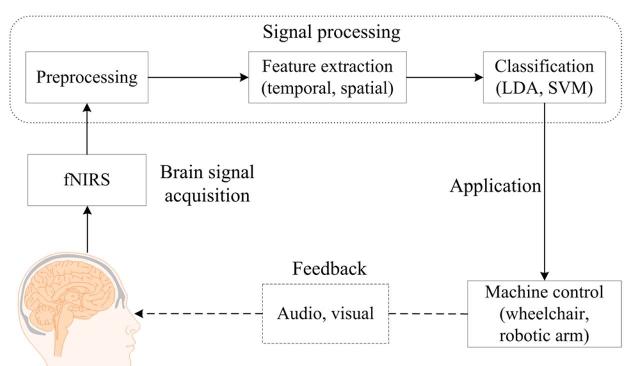

Fig. 2 Block diagram of a typical fNIRS-based BMI

in HR through initial dip, will also be discussed in later sections [56–60].

3 BMI modules

As alluded to in the Introduction section, BMIs can be designed with certain key modules. We will broadly discuss these modules in light of fNIRS-based BMI studies along with the necessary support from the literature.

3.1 Brain activity selection

The foremost step is the selection of brain regions from where the signals are generated depending on the corresponding tasks or activities. The signals are generally acquired from the prefrontal and/or motor cortices. The signals corresponding to motor execution and motor imagery tasks can be acquired from the motor cortex, whereas those corresponding to cognitive tasks can be acquired from the prefrontal cortex [61–63]. It is pertinent to mention that the years 2011–2013 can be considered a golden period for fNIRS-based BMIs: approximately 20 studies were published that selected prefrontal and motor cortices of the brain for signal acquisition where different motor and cognitive tasks were presented to subjects [56, 59, 64–79]. The literature suggests that the activity from the motor cortex or the prefrontal cortex is a good choice for fNIRS-based BMIs. Motor execution tasks can be explained as the movement of body parts, such as the finger, hand, arm, or leg, that result in the generation of signals at the motor cortex of the brain. After processing, the signals acquired through fNIRS serve as controlling commands of the external device, which is sometimes not feasible in cases of locked-in patients and PWPD. In this way, an alternate called motor imagery tasks is very handy, which is one of the most commonly employed tasks in fNIRS-BMI. As the name suggests, it is a motor function-related activity without actual movement of one's own body part, i.e., the imagination of movement. This activity usually appears in the premotor cortex and, as evidence suggests, the prefrontal cortex [80]. Many cognitive tasks, such as object rotation, music imagery, mental arithmetic, change detection, mental singing, emotionally rated music listening, verbal fluency, word formation, puzzle-solving, happy thoughts, Stroop tasks, future visualization, focus on a screen, and imagination of pictures are responsible for generating activity in the prefrontal cortex of the brain [11]. Activities from the prefrontal cortex are beneficial, especially in the case of locked-in patients as well as patients in a vegetative state where the motor cortex is not working. It was recently demonstrated that eleven different patterns of activity could be decoded from the prefrontal cortex [81]. Studies in the field of fNIRS have also demonstrated its advantage in monitoring passive activities, such as drowsiness detection and working memory, for the purpose of passive BMIs [15, 82].

Another important step is the positioning of fNIRS optodes (illuminators and detectors) atop the subject heads. Usually, the optodes are placed around the brain using the International 10/20 or 10/10 EEG electrode placement system [83]. It is important to place optodes at specific locations to obtain maximum fNIRS measurements; usually, 2.5–3 cm distances are recommended [84–86]. Various optode arrangements can be made on desired brain areas; for example, a more than 5 cm separation might result in weak signals, while less than 1 cm distance may contain artifacts from skin-scalp contributions. However, the latest studies show promising results by incorporating short separation (0.8–1 cm apart) channels for the removal of cortical noise [87–91]. Another aspect is the sufficient number of illuminators/detector pairs for adequate extraction of neuronal activity. This number varies depending on the type of brain signals (motor or cognitive) that can be used for BMI purposes. For obtaining cognitive measurements from the prefrontal cortex, three illuminators and eight detectors may be sufficient for an adequate amount of brain signals [52, 53, 74]. Several configurations of fNIRS optodes have been used in obtaining brain activities corresponding to motor tasks for BMIs, such as six and four pairs of optodes or four illuminators and ten detectors, which can cover the entire cortex [47, 92–94].

3.2 Preprocessing

After selection of the brain region for the acquisition of signals corresponding to a particular activity and the correct positioning of optodes over the subject's head, the obtained signals are then processed to obtain relevant information that can be used for communication and control. It is likely that the acquired signals may contain different kinds of noise, such as instrumental noise, physiological noises, and experimental error [6, 41, 95–97]. Instrumental noise is the noise found in fNIRS signals generated either by hardware or from the surrounding environment. Instrumental degradation can be considered as an example. It commonly involves high (constant) frequencies that can be removed by a low-pass filter. Likewise, by minimizing the variation of external lights, instrument noise can be significantly reduced. Experimental errors include motion artifacts, i.e., head motions, which cause the movement of optodes from their assigned positions. This can cause a sudden change in the light intensity, resulting in spike-like noise. Various filters have been applied in the past to eliminate experimental-related errors, such as Savitzky–Golay filters, Wavelet analysis-based methods, Wiener filtering, and eigenvector-based spatial filtering [53, 77, 98, 99]. Since instrumental noise and experimental errors are not related to brain activity, it is better to remove them prior to converting the raw optical density signals to the concentration changes of ΔHbO and ΔHbR through the modified Beer–Lambert law [100]. Physiological noises include those due to circulation, respiration, and Mayer waves, which are related to blood pressure fluctuations. In signal preprocessing, these noises are removed from the converted data, i.e., the concentration changes of hemoglobin. Various methods have been applied to remove physiological noise from the data in the studies alluded to above and in later studies, including band-pass filtering, common averaging reference, spatial filtering, adaptive filtering, principal component analysis, and independent component analysis [47, 101–104]. When the frequencies of the physiological noise are known, a band-pass filter can serve the purpose of removing them. Conversely, respiration-related noise may not be removed using band-pass filtering, and then adaptive filtering can be applied. Independent and principal component analyses are helpful in determining when to separate physiological noises from the mixed signals that ultimately provide the desired HR. Many fNIRS-based BMI studies have used these filters for the removal of unnecessary noise [105–108]. However, the advantage of a particular noise removal technique over others has not yet been reported.

3.3 Features and classification

After preprocessing—in other words, the removal of noise—the specific characteristics of signals, known as features, are acquired for translation into control commands. An important aspect of acquiring features is to define the size of a time window that is most suitable for acquiring features for the generation of control commands. Due to the delayed nature of hemodynamic signals, features have been mostly selected in time ranges of 0–5, 2–7, 0–10, 0–15, 0–17, or 0–20 s windows [6, 15, 94]. It is not unusual to select a larger window size depending on the length of the stimulation, but for a 10 s stimulation task, a 2–7 s time window may provide better results [109]. Once the time window is selected, features can be extracted from the signals for further processing.

In fNIRS-based BMIs, primarily hemodynamic signals have been used for the extraction of certain features [110]. Additionally, the literature indicates that light intensity signals have also been used for the acquisition of appropriate features [52, 53]. In comparison to light intensity signals, more options are available in the selection of suitable features from various hemodynamic signals that include HbO, HbR, total hemoglobin (HbT), and cerebral oxygen exchange (COE = HbO–HbR). Better results in classifying these signals can be achieved by obtaining optimal feature sets that are similar to a certain class and different from others. In past BMI studies, many features, such as the mean HbO, mean HbR, skewness, kurtosis, variance, zero crossings, decomposed intrinsic mode functions, slope, number of peaks, sum of peaks, and peak values, were computed from specific time windows for classification [47, 51, 58, 74, 111–113]. Moreover, different combinations of such features may provide the necessary discriminatory information for the purpose of classification [114]. Most of these features can be obtained using built-in functions in MATLAB™; the definitions of these features in the form of equations can be found in the literature [15]. Recently, studies have shown the use of HbT and COE for initial dip detection, which can be used as a feature for quicker command generation [115, 116].

Classification techniques are used to identify the different brain signals generated by the user. These identified signals are then translated into control commands for application interface purposes. In most existing fNIRS-BMIs, such identification is performed using classification techniques to discriminate various brain signals based on appropriate features. These classifiers can be termed discrete classifiers, which convert neuronal activities into discrete choices. Since the user can generate a limited number of commands in noninvasive BMIs, these types of discrete classifiers are commonly used. Such classification algorithms, calibrated by supervised learning during a training phase, can detect brain-signal patterns during the testing stage. Some of the more commonly used mathematical algorithms in fNIRS-BMIs for discrete classification purposes include LDAs, SVMs, HMM, heuristic search algorithms, extreme learning machines, and artificial neural networks (ANNs) [15, 61, 117–119]. Although SVM, ANN, and HMM showed better performance due to their inherent nature of nonlinearity, for BMI applications, it is useful to deploy classifiers that must be fast and accurate. Thus, LDA, due to its simple structure and low computational cost, has been widely used. The mathematics involved in these classification algorithms can be obtained from the literature [11].

Figure 3 shows pie charts illustrating the distribution of features and classifiers that have been used in the literature (2010–2019, 74 articles). This will be helpful for research groups in the BMI field to select proper features from fNIRS signals and classifiers.

4 Applications

The core purpose of BMIs is to communicate with PWPD or patients with persistent locked-in syndrome, which is not achievable in the absence of an absolute interface with a machine. Therefore, after classification, the generated command signals are sent to the external interfaces for communication. It is difficult for PWPD to generate multiple commands to operate complex systems. Therefore, fNIRS-based BMIs must be designed with respect to the numbers of

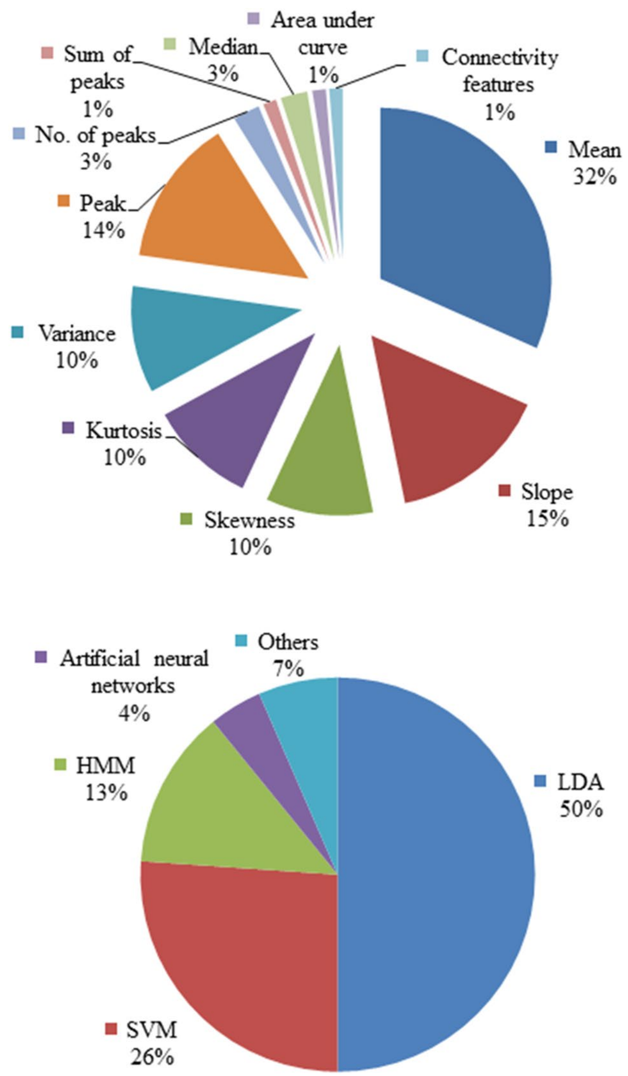

Fig. 3 Features (upper panel) and classifiers (lower panel) used in fNIRS-based BMI studies. The charts were constructed using 74 articles (2010–2019) from Web of Science (https://www.isiknowledge.com)

commands that the end-user can generate. Researchers have developed an fNIRS-BMI system for binary communication based on activation from the prefrontal area [106]. The subjects were asked to perform a specific task such as mental arithmetic or music imagery to increase the cognitive load and thereby respond "yes," or to remain relaxed and thus respond "no", to the given question. Gallegos-Ayala et al. reported on an fNIRS-based BMI system for a patient with ALS who answered different questions by simply thinking 'yes' or 'no', which resulted in an online classification accuracy of ~ 72% [35]. Hwang et al. tested a similar paradigm on eight healthy participants that resulted in an offline average accuracy of ~ 76% when the best feature set was employed for each participant [120]. Astonishingly, the fNIRS channel locations did not cover the temporal regions, which are mostly considered important speech-related brain areas. In [34], Chaudhary et al. extended the work presented in [35] by increasing the number of ALS patients to four and thus achieved an average online classification accuracy of more than ~ 70%. Another notable study by Abdalmalak et al. reported the feasibility of a time-resolved system, which was tested to communicate with a patient with Guillain–Barre syndrome, without the need for prior training, for the establishment of an fNIRS-based BMI system [36].

In another study, a less restrictive and stable measurement system for BMIs for second language learning was proposed, which resulted in the creation of the Yerkes–Dodson law [121]. An fNIRS-based BMI was demonstrated as a new type of neural prosthetic system for helping locked-in syndrome patients by identifying/reconstructing speech with a machine algorithm that achieved average classification accuracies of ~ 75% and ~ 44% for 50-s- and 25-s-long stories, respectively [122]. Moreover, some studies have shown the ability to classify multiple commands simultaneously from two different regions of the brain [109]. In addition, a 3-class online fNIRS-based imagined speech BMI has been demonstrated using regularized LDA by optimizing its parameters during the study, which resulted in an accuracy of ~ 84% for 9 out of 12 subjects [123].

fNIRS is more attractive than fMRI with regard to accessing subcortical brain signals because of its low cost, user-friendliness, and portability. Most of its appeal, however, is in its lower susceptibility to motion artifacts. Given the above points, the potential uses of fNIRS in neurofeedback studies are numerous [110]. Using neurofeedback, the induction of neuroplasticity in selected brain areas can be accomplished, which has the potential to improve cognitive performance. A study aimed at developing a synchronous fNIRS-based BMI paradigm using an action observation task that represents a neural activity comprised of imagining movement while watching a complex motor action and empirical analysis was able to decode these tasks with reasonable accuracy as BMI commands [124, 125]. In another study, the possibility of using neurofeedback that allows users to deliberately regulate their own brain function corresponding to a motor imagery task was presented. These results were further replicated in Stroke patients [126]. Similarly, another study was conducted to check the effect of feedback while imagining squeezing an elastic ball that resulted in modulation of activity [127]. Yet another study explored the affective engagement of subjects with a virtual agent as neurofeedback [128]. Recently, a toolbox named Turbo-Satori was designed for real-time applications of fNIRS-based BMIs with neurofeedback [129].

Though the use of fNIRS in BMIs is still emerging, it has shown potential as a supplement or replacement for electroencephalography for the restoration of movement capabilities for PWPD. The control commands generated by a BMI system can be used to control a prosthetic limb or a wheelchair. A study has demonstrated the first online results of four motor-imagery tasks (left hand, right hand, left foot, and right foot) mapped to four high-level commands (turn left/right, move forward/backward) to control the navigation of a virtual avatar or a DARwIn-OP humanoid robot; the classification accuracy during the control of original robot was significantly improved [130]. However, most fNIRS studies have not yet provided a device interface, such as the wheelchair, that can prove its utility for patients. Additionally, it is desirable to have a portable system for these applications so that the user can move freely [131]. Moreover, these applications, for safety purposes, cannot afford high error rates and must be fast enough to provide real-time control. Several fNIRS-based BMI studies have tried to improve classification accuracies using adaptive algorithms and to enhance information transfer rates [132, 133]. A Gaussian mixture model and general linear model-based adaptive algorithms were applied to enhance classification accuracy [134, 135]. A common spatial pattern-based algorithm has also been used to improve the average accuracies [136].

5 Challenges

It can be concluded from the discussion above that we are still far from successfully implementing a BMI for PWPD in real-time. Nevertheless, current research is heading in the right direction, and consequently, the desired goals may be achievable. Some key issues still need to be resolved before progressing towards achieving these goals.

The first shortcoming in current research on BMIs is the lack of patients' inclusion in the experiments. A large body of fNIRS-based BMI research uses healthy subjects, which creates a translation gap from proof of concept to actual implementations. Successful results from healthy people may not reflect the achievement of the same outcomes in patients.

The selection of suitable brain activity for patients is the second essential factor for BMIs. Based on the presently available literature, we have no confidence to say which brain task is the most appropriate for a patient. Although a healthy person can perform any rational task, a patient may need various options to choose the appropriate one. A robust conclusion can only be achieved if a sufficient number of patients are used in BMI studies for evaluating various brain tasks.

The third concern is the selection of a suitable brain region. As alluded to in the preceding sections, a consensus has not yet been achieved on using one or two appropriate regions for patients. However, this decision may vary depending on the specific patient case. Additionally, most studies either use averaging of fNIRS channels or rely only on a single channel for BMIs, but a precise positioning of optodes on the brain is required for high-quality detection of activity.

One more issue with current fNIRS studies is the lack of physical implementation of BMIs. Additional sensors, such as those monitoring blood pressure and respiration, may be helpful in generating correct commands with BMI realization. Due to the incorrect generation of commands, the outcome may be severe in real-time scenarios with locked-in patients, even in binary decoding. Thus, expansion in this category is necessary.

Other challenges are the lower number of commands and command generation time, assuming the above issues are fully addressed. A definite number of commands are essential for the accurate operation of BMI systems, but increasing the number of commands will reduce the classification accuracy and thus reduce the decoding ability. Therefore, in the following section, we will review some methods and techniques used to increase the number of commands and reduce command generation time, along with the inclusion of some noninvasive techniques of brain therapy for modulation of brain activities.

6 Current trends

Current trends in fNIRS are now moving towards hybridization, reduction in command generation time with the help of initial dip techniques, and noninvasive brain therapies such as transcranial direct current stimulation (tDCS) or repetitive transcranial magnetic stimulation (rTMS). In the next subsections, we will briefly overview the advantages of hybrid systems in light of improvements in BMI applications. We will also summarize the notable findings of hybrid systems in tabular form. Furthermore, studies involved in reducing command generation time will be discussed along with stimulation therapy that can be used for enhancement of cortical activities.

6.1 Hybrid systems

In literature covering BMIs or BCIs, it can be inferred that the output from hemodynamics is sufficient to control external devices. Conversely, the obtained high accuracy may be due to the false detection of hemodynamic signals or the bias of fewer participants in the study. In real-time cases, this incorrect judgment may become a problem for patients from a safety point of view. For this reason, a hybrid system approach, specifically the combination of hemodynamic signals (fNIRS) and neuronal signals (EEG), may be useful. Although research on concurrent fNIRS-EEG measurements is very limited, the obtained results are improved in terms of increased classification or a higher number of control

Table 1 Hybrid fNIRS-EEG Brain–machine interface studies with applications to increased accuracy (from 2012 to 2019)

Authors	Brain area	Task	EEG feature	fNIRS feature	Classifier	Accuracy
Fazli et al. [37]	Frontal, sensorimotor, and parietal	Motor execution and imagery	Band power	Mean ΔHbO, ΔHbR and ΔHbT	LDA	> 90
Kaiser et al. [137]	Sensorimotor	Motor imagery		Mean ΔHbO		≤ 70%
Tomita et al. [38]	Occipital	Flickering visual stimuli	SSVEP	First and second derivatives of the difference of ΔHbO and ΔHbR	Joint classifier	Improvement in error rates 85%
Khan et al. [92]	fNIRS: prefrontal EEG: sensorimotor	Mental arithmetic and motor imagery	Peak amplitudes	Mean values of ΔHbO and ΔHbR	LDA	> 80%
Blokland et al. [138]	Sensorimotor	Motor imagery and attempt	Power spectral features in 0 ~ 15 s window	Mean of HbO and HbR in 3 ~ 18 s window	Linear logistic regression classifier	Average accuracy = ~ 78%
Putze et al. [139]	fNIRS: Temporal and occipital EEG: whole scalp	Audio and video perception	Event-related potential and band power changes	Difference of mean of HbO and HbR	SVM	> 90%
Morioka et al. [140]	fNIRS: parietal and occipital EEG: Whole scalp	Spatial attention	Alpha and beta bands	Mean of HbO		~ 79%
Koo et al. [141]	Sensorimotor	Motor imagery	Alpha band power	Threshold for HbO	SVM	True positive rate of 88%
Yin et al. [142]			Time–frequency Phase	Difference of HbO and HbR	ELM	~ 89%
Lee et al. [143]		Motor imagery with visual feedback	Common spatial pattern and Log variance	Mean amplitudes of ΔHbO and ΔHbR	LDA	~ 59%
Buccino et al. [144]		Motor execution	Common spatial pattern	Mean and slope of HbO		~ 70%
Ahn et al. [145]	fNIRS: prefrontal EEG: whole scalp	Simulated driving	Alpha/beta band power	Amplitude of HbO and HbR		~ 68%
Khan and Hong [39]	Prefrontal	Mental task	Mean and number of peaks	Peak and mean of ΔHbO and Initial dip features (minimum value in 2 s window)		~ 76%
Li et al. [146]	Sensorimotor	Motor execution	Coefficient of wavelet transform	Mean values of HbO and HbR in 2 s window	SVM	~ 91%
Aghajani et al. [147]	Prefrontal	Working memory	Band power and phase locking value	Peak, slope, standard deviation, skewness and kurtosis of HbO and HbR		> 80%
Liu et al. [148]	fNIRS: prefrontal EEG: whole scalp	Working memory	Bands power	Mean amplitude of ΔHbO and ΔHbR	LDA	~ 72%
Shin et al. [149]	fNIRS: prefrontal EEG: whole scalp	Stroop and mental arithmetic task	Log-scaled variance	Mean values and average slope of ΔHbO and ΔHbR	Shrinkage LDA	~ 88%
Omurtag et al. [150]	fNIRS: prefrontal EEG: whole scalp	Category fluency task	Band power and phase locking value	Mean values and correlation of ΔHbO and ΔHbR	SVM	~ 90%
Zhang et al. [151]	Sensorimotor	Fisting action task	Wavelet Coefficient	Slope of ΔHbO	SVM	~ 83%

Table 1 (continued)

Authors	Brain area	Task	EEG feature	fNIRS feature	Classifier	Accuracy
Chiarelli et al. [152]	fNIRS: motor cortex EEG: whole scalp	Motor imagery	Raw data	Raw ΔHbO and ΔHbR	LDA SVM DNN	~68% ~88% ~94.6%

commands compared to fNIRS- or EEG-only systems. The hybrid fNIRS-EEG system was evolved in 2012, and until 2019–2020 studies have been published specifically for the purpose of developing BMIs [37–39, 92, 137–152]. Summaries of their developments toward BMIs are provided in Table 1. The majority of studies were carried out on healthy people. The simultaneous measurement of fNIRS with other biosignals showed promising results. However, for BMI applications, the hybrid fNIRS-EEG is considered best to date. An imperative disadvantage of using hemodynamics (either fMRI or fNIRS) is the inherent delay in its response, which makes the generation of commands slower compared to EEG. However, in the case of combined fNIRS-EEG, this kind of disadvantage can be removed.

6.2 Command generation

As alluded to above, some research issues are still present in fNIRS-based BMIs without the inclusion of additional modalities: (1) improvement in the classification accuracy; (2) increase in the number of commands generated from the brain for external control; and (3) rapid decoding of the command to reduce delays. In 2016, a study was conducted to improve the vector phase diagram by incorporating a threshold circle with a radius of $\max(\Delta\mathrm{HbO}^2 + \Delta\mathrm{HbR}^2)^{1/2}$ during the resting state. This was used as a decision criterion for the occurrence of an initial dip, thereby reducing the detection time to approximately 0.9 s [115]. The next year, this work was extended by Zafar and Hong, in which they used the same methodology and modified the radius of the threshold circle to $\max\{\Delta\mathrm{HbO}, \Delta\mathrm{HbR}\}$, which was further applied to the classification problem of three cognitive tasks for BMIs [116]. They revealed a reduction in the time of command generation to 2.5 s for fNIRS-based BMIs. However, a limitation persisted in the form of detecting false dips. This limitation was addressed recently in their extended work by adding second threshold criteria that can be applied for BMIs with an increased number of commands from a wider brain region [153]. This was achieved using a dense optode configuration of fNIRS channels over the brain. As explained in the previous section, the present fNIRS-based BMI framework uses HR features only, but after developments in the initial dip, these features can be extracted in time windows of 0 – 2 s or 0 – 2.5 s. Population-level feature sets were also used recently to improve the classification accuracy of fNIRS-based BMIs [154]. Early command generation using hybrid modalities with vector phase analysis as a classifier showed great improvement in classification accuracy compared to conventional classifiers in a window of 0–1.5 s [155]. Figure 4 shows the improved fNIRS-based BMI model for quicker command generation and brain function recovery using noninvasive stimulation techniques.

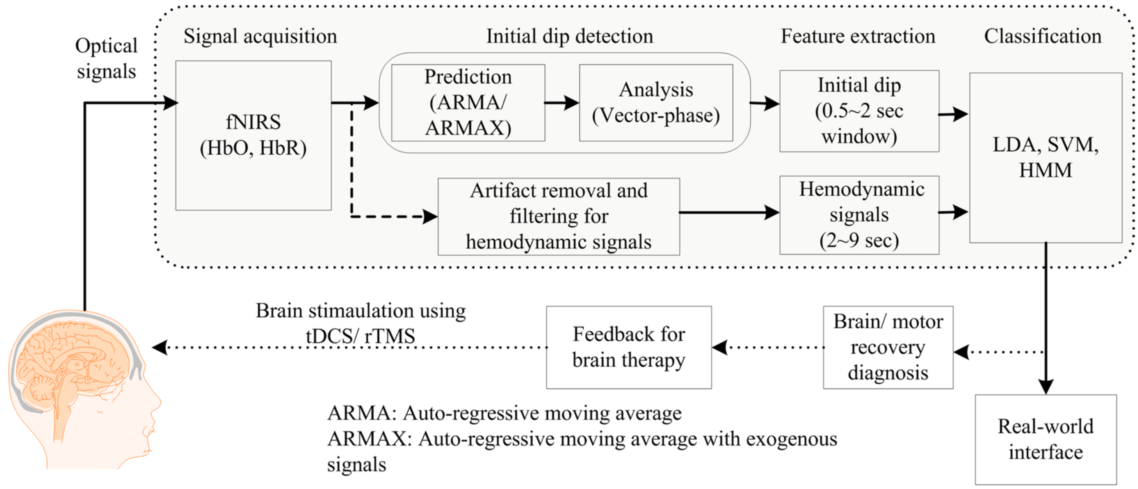

Fig. 4 Improved fNIRS-based BMI framework: (i) initial-dip features for quick command generation, and (ii) brain function recovery by application of non-invasive stimulation (inspired by Hong et al. [11])

6.3 Brain stimulation and mapping

Identification of a precise brain area for stimulation is important for brain therapy, and fNIRS has the advantage of identifying such areas. Research with bundled optode configurations has shown the ability of fNIRS to differentiate brain areas for different finger movements [87]. Furthermore, brain therapy is an essential factor when brain activity detection is not workable and in the quest to improve the state of the brain. Thus, combining rTMS, tDCS, or manual acupuncture with fNIRS can improve the brain therapy process, which further enhances brain activity [156, 157]. This may lead to improve motor recovery for stroke patients or cognitive function of mild cognitive impairment patients [158, 159]. A proposed feedback control scheme for brain stimulation and motor/cognitive recovery is shown in Fig. 5. This figure shows that the desired brain output can be achieved by stimulating the brain using external actuators. In the case of the human brain, the actuators can be rTMS-, tDCS- or ultrasound-based devices that can stimulate the brain according to the sensor data. The sensor or monitoring device can be an fNIRS system from which a brain diagnosis can be made.

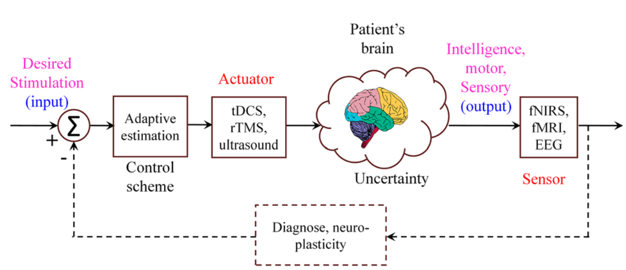

Fig. 5 Feedback control strategy of the brain

Along with the above-mentioned methods, the most important need for current fNIRS-based BMI systems is to apply them to real patients. Additionally, there is a need to develop the hardware of either single or dual modality that must be portable and comfortable for patients in real-time BMI applications [33, 131, 160, 161]. Single-trial classifications can be improved with the help of newly adopted graph signal processing and adaptive algorithms [162–164]. In addition, further research on the bundled optode scheme using fNIRS is required to narrow down the optimal brain region for patients [87, 165]. Indeed, EEG signals represent attenuated and filtered brain activity, which in turn represents the population activity produced by many millions of neurons. These EEG signals lack fine spatial resolution and do not provide precise task-related neuronal signals that can be refined by integrating fNIRS for BMI applications.

7 Conclusion

In this study, we presented an overview of the development of a functional near-infrared spectroscopy-based Brain–machine interface. We briefly discussed the development of fNIRS-based BMIs in terms of preprocessing, feature extraction, and classification. The role of fNIRS in hybridization and brain therapy was also discussed. Although fNIRS-based BMI applications for communication and control have been demonstrated in a number of studies, there is no commercially available system that can be used for the treatment of stroke and locked-in patients. With the most recent advancement in brain stimulation and therapy, research on fNIRS-based BMI systems is expected to grow. All of the relevant research trends predict that fNIRS-based systems may create a breakthrough in the area of brain diagnosis for locked-in patients.

Acknowledgements This work was supported in part by the National Research Foundation (NRF) of Korea under the auspices of the Ministry of Science and ICT, Republic of Korea (Grant no. NRF-2017R1A2A1A17069430).

Compliance with ethical standards

Conflict of interest The authors declare that they have no conflict of interest. This research was conducted in the absence of any commercial or financial relationship that could be construed as a potential conflict of interest.

References

1. Wolpaw JR, Birbaumer N, McFarland D, Pfurtscheller G, Vaughan TM (2002) Brain–computer interfaces for communication and control. Clin Neurophysiol 113(6):767–791
2. Moghimi S, Kushki A, Marie Guerguerian A, Chau T (2013) A review of EEG-based brain–computer interfaces as access pathways for individuals with severe disabilities. Assist Technol 25(2):99–110
3. Eddy BS, Garrett SC, Rajen S, Peters B, Wiedrick J, McLaughlin D, O'Connor A, Renda A, Huggins JE, Fried-Oken M (2019) Trends in research participant categories and descriptions in abstracts from the international BCI meeting series, 1999 to 2016. Brain Comput Interface 6(1–2):13–24
4. https://www.un.org/en/development/desa/population/publications/pdf/ageing/WPA2015_Report.pdf. Accessed Dec 2016
5. Nicolas-Alonso LF, Gomez-Gil J (2012) Brain–computer interfaces, a review. Sensors 12(2):1211–1279
6. Naseer N, Hong KS (2015) fNIRS-based brain–computer interfaces: a review. Front Hum Neurosci 9:3
7. Birbaumer N (2006) Brain computer-interface research: coming of age. Clin Neurophysiol 117(3):479–483
8. Birbaumer N, Cohen LG (2007) Brain computer interfaces: communication and restoration of movement in paralysis. J Physiol 579:621–636
9. Sitaram R, Caria A, Birbaumer N (2009) Hemodynamic brain–computer interfaces for communication and rehabilitation. IEEE Trans Neural Netw Learn Syst 22(9):1320–1328
10. Min BK, Marzelli MJ, Yoo SS (2010) Neuroimaging-based approaches in brain–computer interface. Trends Biotechnol 28:552–560
11. Hong KS, Khan MJ, Hong MJ (2018) Feature extraction and classification methods for hybrid fNIRS-EEG brain–computer interfaces. Front Hum Neurosci 12:246
12. Birbaumer N, Ghanayim N, Hinterberger T, Iversen I, Kotchoubey B, Kubler A, Perelmouter J, Taub E, Flor H (1999) A spelling device for the paralysed. Nature 398:297–298
13. Chapin JK, Moxon KA, Markowitz RS, Nicolelis MA (1999) Real-time control of a robot arm using simultaneously recorded neurons in the motor cortex. Nat Neurosci 2:664–670
14. Vidal JJ (1973) Toward direct brain–computer communication. Annu Rev Biophys Bioeng 2:157–180
15. Khan MJ, Hong KS (2015) Passive BCI based on drowsiness detection: an fNIRS study. Biomed Opt Express 6(10):4063–4078
16. Bashashati A, Fatourechi M, Ward RK, Birch GE (2007) A survey of signal processing algorithms in brain–computer interfaces based on electrical brain signals. J Neural Eng 4(2):R32–R57
17. Lotte F, Congedo M, L´ecuyer A, Lamarche F, Arnaldi B (2007) A review of classification algorithms for EEG-based brain–computer interfaces. J Neural Eng 4(2):R1–R13
18. Trejo LJ, Rosipal R, Matthews B (2006) Brain–computer interfaces for 1-D and 2-D cursor control: designs using volitional control of the EEG spectrum or steady-state visual evoked potentials. IEEE Trans Neural Syst Rehabil Eng 14:225–229
19. Wang D, Miao DQ, Blohm G (2012) Multi-class motor imagery EEG decoding for brain–computer interfaces. Front Neurosci 6:151
20. Turnip A, Hong KS (2012) Classifying mental activites from EEG-P300 signals using adaptive neural network. Int J Innov Comp Inf Control 8(9):6429–6443
21. Turnip A, Hong KS, Jeong MY (2011) Real-time feature extraction of EEG-based P300 using adaptive nonlinear principal component analysis. Biomed Eng Online 10(83):1–20
22. Ahn M, Jun SC (2015) Performance variation in motor imagery brain–computer interface: a brief review. J Neurosci Methods 243:103–110
23. Wang HT, Li YQ, Long JY, Yu TY, Gu ZH (2014) An asynchronous wheelchair control by hybrid EEG-EOG brain–computer interface. Cogn Neurodyn 8:399–409
24. Ramli R, Arof H, Ibrahim F, Mokhtar N, Idris MYI (2015) Using finite state machine and a hybrid of EEG signal and EOG artefacts for an asynchronous wheelchair navigation. Expert Syst Appl 42:2451–2463
25. Zhang R, Li YQ, Yan YY, Zhang H, Wu SY, Yu TY, Gu ZH (2016) Control of a wheelchair in an indoor environment based on a brain–computer interface and automated navigation. IEEE Trans Neural Syst Rehabil Eng 24:128–139
26. Kim BH, Kim M, Jo S (2014) Quadcopter flight control using a low-cost hybrid interface with EEG-based classification and eye tracking. Comput Biol Med 51:82–92
27. Boas DA, Elwell CE, Ferrari M, Taga G (2014) Twenty years of functional near-infrared spectroscopy: introduction for the special issue. Neuroimage 85:1–5
28. Liu X, Hong KS (2017) Detection of primary RGB colors projected on a screen using fNIRS. J Innov Opt Health Sci 10:6
29. Bhutta MR, Hong MJ, Kim YH, Hong KS (2015) Single-trial lie detection using a combined fNIRS-polygraph system. Front Psychol 6:709
30. Scholkmann F, Kleiser S, Metz AJ, Zimmermann R, Pavia JM, Wolf U, Wolf M (2014) A review on continuous wave functional near-infrared spectroscopy and imaging instrumentation and methodology. Neuroimage 85:6–27
31. Huppert TJ, Hoge RD, Diamond SG, Franceschini MA, Boas DA (2006) A temporal comparison of BOLD, ASL, and NIRS hemodynamic responses to motor stimuli in adult humans. Neuroimage 29(2):368–382
32. Hu XS, Hong KS, Ge SS, Jeong MY (2010) Kalman estimator- and general linear model-based on-line brain activation mapping by near-infrared spectroscopy. Biomed Eng Online 9:82
33. Pinti P, Aichelburg C, Gilbert S, Hamilton A, Hirsch J, Burgess P, Tachtsidis I (2018) A review on the use of wearable functional near-infrared spectroscopy in naturalistic environments. Jpn Psychol Res 60(4):347–373
34. Chaudhary U, Xia B, Silvoni S, Cohen LG, Birbaumer N (2017) Brain–computer interface–based communication in the completely locked-in state. PLoS Biol 15(1):1002593
35. Gallegos-Ayala G, Furdea A, Takano K, Ruf CA, Flor H, Birbaumer N (2014) Brain communication in a completely locked-in patient using bedside near-infrared spectroscopy. Neurology 82(21):1930–1932
36. Abdalmalak A, Milej D, Norton L, Debicki D, Gofton T, Diop M, Owen AM, Lawrence KS (2017) Single-session communication

with a locked-in patient by functional near-infrared spectroscopy. Neurophotonics 4(4):040501
37. Fazli S, Mehnert J, Steinbrink J, Curio G, Villringer A, Muller KR, Blankertz B (2012) Enhanced performance by a hybrid NIRS-EEG brain computer interface. Neuroimage 59:519–529
38. Tomita Y, Vialatte FB, Dreyfus G, Mitsukura Y, Bakardjian H, Cichocki A (2014) Bimodal BCI using simultaneosuly NIRS and EEG. IEEE Trans Biomed Eng 61(4):1274–1284
39. Khan MJ, Hong KS (2017) Hybird EEG-fNIRS-based eight command decoding for BCI: application to quadcopter control. Front Neurorobotics 11:6
40. Hong KS, Khan MJ (2017) Hybrid brain–computer interface techniques for improved classification accuracy and increased number of commands: a review. Front Neurorobotics 11:35
41. Santosa H, Hong MJ, Hong KS (2014) Lateralization of music processing with noises in the auditory cortex: an fNIRS study. Front Behav Neurosci 8:418
42. Hong KS, Bhutta MR, Liu X, Shin YI (2017) Classification of somatosensory cortex activities using fNIRS. Behav Brain Res 333:225–234
43. Naseer N, Hong KS (2015) Decoding answers to four-choice questions using functional near-infrared spectroscopy. J Near Infrared Spectrosc 23(1):23–31
44. Jobsis FF (1977) Noninvasive, infrared monitoring of cerebral and myocardial oxygen sufficiency and circulatory parameters. Science 198:1264–1267
45. Coyle SM, Ward TE, Markham CM, McDarby G (2004) On the suitability of near-infrared (NIR) systems for next-generation brain–computer interfaces. Physiol Meas 25(4):815
46. Coyle SM, Ward TE, Markham CM (2007) Brain–computer interface using a simplified functional near-infrared spectroscopy system. J Neural Eng 4(3):219
47. Sitaram R, Zhang H, Guan C, Thulasidas M, Hoshi Y, Ishikawa A, Shimizu K, Birbaumer N (2007) Temporal classification of multichannel near-infrared spectroscopy signals of motor imagery for developing a brain–computer interface. Neuroimage 34(4):1416–1427
48. Naito M, Michioka Y, Ozawa K, Ito Y, Kiguchi M, Kanazawa T (2007) A communication means for totally locked-in ALS patients based on changes in cerebral blood volume measured with near-infrared light. IEICE Trans Inf Syst 90(7):1028–1037
49. Utsugi K, Obata A, Sato H, Aoki R, Maki A, Koizumi H, Sagara K, Kawamichi H, Atsumori H, Katura T (2008) GO-STOP control using optical brain–computer interface during calculation task. IEICE Trans Commun 91(7):2133–2141
50. Bauernfeind G, Leeb R, Wriessnegger SC, Pfurtscheller G (2008) Development, set-up and first results for a one-channel near-infrared spectroscopy system. Biomed Tech 53(1):36–43
51. Tai K, Chau T (2009) Single-trial classification of NIRS signals during emotional induction tasks: towards a corporeal machine interface. J NeuroEng Rehabil 6(1):39
52. Luu S, Chau T (2009) Decoding subjective preference from single-trial near-infrared spectroscopy signals. J Neural Eng 6(1):016003
53. Power SD, Falk TH, Chau T (2010) Classification of prefrontal activity due to mental arithmetic and music imagery using hidden Markov models and frequency domain near-infrared spectroscopy. J Neural Eng 7(2):026002
54. Cui X, Bray S, Reiss AL (2010) Speeded near infrared spectroscopy (NIRS) response detection. PLoS ONE 5(11):15474
55. Coffey EB, Brouwer AM, Wilschut ES, van Erp JB (2010) Brain–machine interfaces in space: using spontaneous rather than intentionally generated brain signals. Acta Astronaut 67(1–2):1–11
56. Power SD, Khushki A, Chau T (2012) Automatic single-trial discrimination of mental arithmetic, mental singing and no-control state form the prefrontal activity: towards the three state NIRS-BCI. BMC Res Notes 5:141
57. Pfurtscheller G, Allison BZ, Bauernfeind G, Brunner C, Solis Escalante T, Scherer R, Zander TO, Mueller-Putz G, Neuper C, Birbaumer N (2010) The hybrid BCI. Front Neurosci 4:3
58. Hong KS, Zafar A (2018) Existence of initial dip for BCI: an illusion or reality. Front Neurorobotics 12:69
59. Misawa T, Takano S, Shimokawa T, Hirobayashi S (2012) A brain–computer interface for motor assist by the prefrontal cortex. Electron Commun Jp 95(10):1–8
60. McFarland DJ, Wolpaw JR (2011) Brain–computer interfaces for communication and control. Commun ACM 54:660–666
61. Hong KS, Santosa H (2016) Decoding four different sound-categories in the auditory cortex using functional near-infrared spectroscopy. Hear Res 333:157–166
62. Naseer N, Noori FM, Qureshi NK, Hong KS (2016) Determining optimal feature-combination for LDA classification of functional near-infrared spectroscopy signals in brain–computer interface application. Front Hum Neurosci 10:237
63. Pinti P, Cardone D, Merla A (2015) Simultaneous fNIRS and thermal infrared imaging during cognitive task reveal autonomic correlates of prefrontal cortex activity. Sci Rep 5:17471
64. Abibullaev B, An J, Moon JI (2011) Neural network classification of brain hemodynamic responses from four mental tasks. Int J Optomechatronics 5(4):340–359
65. Abibullaev B, An J (2012) Classification of frontal cortex hemodynamic responses during cognitive tasks using wavelet transforms and machine learning algorithms. Med Eng Phys 34(10):1394–1410
66. Holper L, Wolf M (2011) Single-trial classification of motor imagery differing in task complexity: a functional near-infrared spectroscopy study. J Neuroeng Rehabil 8:34
67. Tanaka H, Katura T (2011) Classification of change detection and change blindness from near-infrared spectroscopy signals. J Biomed Opt 16(8):087001
68. Bauernfeind G, Scherer R, Pfurtscheller G, Neuper C (2011) Single-trial classification of antagonistic oxyhemoglobin responses during mental arithmetic. Med Biol Eng Comput 49(9):979–984
69. Power SD, Kushki A, Chau T (2011) Towards a system-paced near-infrared spectroscopy brain–computer interface: differentiating prefrontal activity due to mental arithmetic and mental singing from the no-control state. J Neural Eng 8(6):066004
70. Chan J, Power S, Chau T (2012) Investigating the need for modeling temporal dependencies in a brain–computer interface with real-time feedback based on near infrared spectra. J Near Infrared Spectrosc 20(1):107–116
71. Seo Y, Lee S, Koh D, Kim BM (2012) Partial least squares-discriminant analysis for the prediction of hemodynamic changes using near-infrared spectroscopy. J Opt Soc Korea 16(1):57–62
72. Power SD, Kushki A, Chau T (2012) Intersession consistency of single-trial classification of the prefrontal response to mental arithmetic and the no-control state by NIRS. PLoS ONE 7(7):37791
73. Falk TH, Guirgis M, Power S, Chau TT (2011) Taking NIRS-BCIs outside the lab: towards achieving robustness against environment noise. IEEE Trans Neural Syst Rehabil Eng 19(2):136–146
74. Stangl M, Bauernfeind G, Kurzmann J, Scerer R, Neuper C (2013) A hemodynamic brain–computer interface based on real-time classification of near infrared spectroscopy signals during motor imagery and mental arithmetic. J Near Infrared Spectrosc 21(3):157–171
75. Naseer N, Hong KS (2013) Classification of functional near-infrared spectroscopy signals corresponding to right- and left-wrist motor imagery for development of a brain–computer interface. Neurosci Lett 553:84–89

76. Zimmermann R, Marchal-Crespo L, Edelmann J, Lambercy O, Fluet MC, Riener R, Wolf M, Gassert R (2013) Detection of motor execution using hybrid fNIRS-biosignal BCI: a feasibility study. J Neuroeng Rehabil 10:4
77. Hai NT, Cuong NQ, Khoa TQD, Toi VV (2013) Temporal hemodynamic classification of two hands tapping using functional near-infrared spectroscopy. Front Hum Neurosci 7:516
78. Faress A, Chau T (2013) Towards a multimodal brain–computer interface: combining fNIRS and fTCD measurements to enable higher classification accuracy. Neuroimage 77:186–194
79. Moghimi S, Kushki A, Power S, Guerguerian AM, Chau T (2012) Automatic detection of a prefrontal cortical response to emotionally rated music using multi-channel near-infrared spectroscopy. J Neural Eng 9(2):026022
80. Hatakenaka M, Miyai I, Mihara M, Sakoda S, Kubota K (2007) Frontal regions involved in learning of motor skill—a functional NIRS study. Neuroimage 34:109–116
81. Weyand S, Chau T (2015) Correlates of near-infrared spectroscopy brain–computer interface accuracy in a multi-class personalization framework. Front Hum Neurosci 9:536
82. Zander TO, Kothe C (2011) Towards passive brain–computer interfaces: applying brain–computer interface technology to human-machine systems in general. J Neural Eng 8:025005
83. Jurcak V, Tsuzuki D, Dan I (2007) 10/20, 10/10, and 10/5 system revisited: their validity as head-surface-based positioning system. Neuroimage 34:1600–1611
84. Tsuzuki D, Dan I (2014) Spatial registration for functional near-infrared spectroscopy: from channel position on the scalp to cortical location in individual and group analyses. Neuroimage 85:92–103
85. Gratton G, Brumback CR, Gordon BA, Pearson MA, Low KA, Fabiani M (2006) Effects of measurement method, wavelength, and source-detector distance on the fast optical signal. Neuroimage 32(4):1576–1590
86. Hu XS, Hong KS, Ge SS (2012) fNIRS-based online deception decoding. J Neural Eng 9(2):026012
87. Nguyen HD, Hong KS, Shin YI (2016) Bundled-optode method in functional near-infrared spectroscopy. PLoS ONE 11(10):0165146
88. Yücel MA, Selb J, Aasted CM, Petkov MP, Becerra L, Borsook D, Boas DA (2015) Short separation regression improves statistical significance and better localizes the hemodynamic response obtained by near-infrared spectroscopy for tasks with differing autonomic responses. Neurophotonics 2(3):035005
89. Hirasawa A, Kaneko T, Tanaka N, Funane T, Kiguchi M, Sørensen H, Secher NH, Ogoh S (2016) Near-infrared spectroscopy determined cerebral oxygenation with eliminated skin blood flow in young males. J Clin Monitor Comp 30(2):243–250
90. Brigadoi S, Cooper RJ (2015) How short is short? Optimum source–detector distance for short-separation channels in functional near-infrared spectroscopy. Neurophotonics 2(2):025005
91. Gao L, Cai Y, Wang H, Wang G, Zhang Q, Yan X (2019) Probing prefrontal cortex hemodynamic alterations during facial emotion recognition for major depression disorder through functional near-infrared spectroscopy. J Neural Eng 16(2):026026
92. Khan MJ, Hong MJ, Hong KS (2014) Decoding of four movement directions using hybrid NIRS-EEG brain–computer interface. Front Hum Neurosci 8:244
93. Aqil M, Hong KS, Jeong MY, Ge SS (2012) Detection of event-related hemodynamic response to neuroactivation by dynamic modeling of brain activity. Neuroimage 63(1):553–568
94. Naseer N, Qureshi NK, Noori FM, Hong KS (2016) Analysis of different classification techniques for two-class functional near-infrared spectroscopy based brain–computer interface. Comput Intell Neurosci 2016:5480760
95. Pinti P, Scholkmann F, Hamilton A, Burgess P, Tachtsidis I (2018) Current status and issues regarding pre-processing of fNIRS neuroimaging data: an investigation of diverse signal filtering methods within a general linear model framework. Front Hum Neurosci 12:505
96. Tachtsidis I, Scholkmann F (2016) False positives and false negatives in functional near-infrared spectroscopy: issues, challenges, and the way forward. Neurophotonics 3(3):031405
97. Bauernfeind G, Wriessnegger SC, Daly I, Müller-Putz GR (2014) Separating heart and brain: on the reduction of physiological noise from multichannel functional near-infrared spectroscopy (fNIRS) signals. J Neural Eng 11(5):056010
98. Cooper RJ, Selb J, Gagnon L, Phillip D, Schytz HW, Iversen HK, Ashina M, Boas DA (2012) A systematic comparison of motion artifact correction techniques for functional near-infrared spectroscopy. Front Neurosci 6:147
99. Ganjefar S, Afshar M, Sarajchi MH, Shao Z (2018) Controller design based on wavelet neural adaptive proportional plus conventional integral-derivative for bilateral teleoperation systems with time-varying parameters. Int J Control Autom Syst 16(5):2405–2420
100. Huppert TJ, Diamond SG, Fransceshini MA, Boas DA (2009) HomER: a review of time-series analysis methods for near-infrared spectroscopy of the brain. Appl Opt 48(10):D280–D298
101. Hu XS, Hong KS, Ge SS (2011) Recognition of stimulus-evoked neuronal optical response by identifying chaos levels of near-infrared spectroscopy time series. Neurosci Lett 504(2):115–120
102. Zhu T, Zhou Y, Xia Z, Dong J, Zhao Q (2018) Progressive filtering approach for early human action recognition. Int J Control Autom Syst 16(5):2393–2404
103. Santosa H, Hong MJ, Kim SP, Hong KS (2013) Noise reduction in functional near-infrared spectroscopy signals by independent component analysis. Rev Sci Instrum 84(7):073106
104. Nguyen QC, Piao M, Hong KS (2018) Multivariable adaptive control of the rewinding process of a roll-to-roll system governed by hyperbolic partial differential equations. Int J Control Autom Syst 16(5):2177–2186
105. Schudlo LC, Chau T (2014) Dynamic topographical pattern classification of multichannel prefrontal NIRS signals: II Online differentiation of mental arithmetic and rest. J Neural Eng 11:016003
106. Naseer N, Hong MJ, Hong KS (2014) Online binary decision decoding using functional near-infrared spectroscopy for the development of brain–computer interface. Exp Brain Res 232(2):555–564
107. Shin J, Jeong J (2014) Multiclass classification of hemodynamic responses for performance improvement of functional near-infrared spectroscopy-based brain–computer interface. J Biomed Opt 19:067009
108. Hwang HJ, Lim JH, Kim DW, Im CH (2014) Evaluation of various mental task combinations for near-infrared spectroscopy-based brain–computer interfaces. J Biomed Opt 19(7):077005
109. Hong KS, Naseer N, Kim YH (2015) Classification of prefrontal and motor cortex signals for three-class fNIRS-BCI. Neurosci Lett 587:87–92
110. Mihara M, Miyai I, Hattori N, Hatakenaka M, Yagura H, Kawano T, Okibayashi M, Danjo N, Ishikawa A, Inoue Y, Kubota K (2012) Neurofeedback using real-time near-infrared spectroscopy enhances motor imagery related cortical activation. PLoS ONE 7(3):32234
111. Herff C, Heger D, Fortmann O, Hennrich J, Putze F, Schultz T (2014) Mental workload during N-back task-quantified in the prefrontal cortex using fNIRS. Front Hum Neurosci 7:935
112. Noori FM, Naseer N, Qureshi NK, Nazeer H, Khan RA (2017) Optimal feature selection from fNIRS signals using genetic algorithms for BCI. Neurosci Lett 647:61–66

113. Yin X, Xu B, Jiang C, Fu Y, Wang Z, Li H, Shi G (2015) NIRS-based classification of clench force and speed motor imagery with the use of empirical mode decomposition for BCI. Med Eng Phys 37(3):280–286
114. Gateau T, Durantin G, Lancelot F, Scannella S, Dehais F (2015) Real-time state estimation in a flight simulator using fNIRS. PLoS ONE 10(3):0121279
115. Hong KS, Naseer N (2016) Reduction of delay in detecting initial dips from functional near-infrared spectroscopy signals using vector-based phase analysis. Int J Neural Syst 26(3):1650012
116. Zafar A, Hong KS (2017) Detection and classification of three-class initial dips from prefrontal cortex. Biomed Opt Express 8:367–383
117. Yin X, Xu B, Jiang C, Fu Y, Wang Z, Li H, Shi G (2015) Classification of hemodynamic responses associated with force and speed imagery for a brain–computer interface. J Med Syst 39(5):53
118. Pamosoaji AK, Piao M, Hong KS (2019) PSO-based minimum-time motion planning for multiple vehicles under acceleration and velocity limitations. Int J Control Autom Syst 17(10):2610–2623
119. Cavazza M, Aranyi G, Charles F (2017) BCI control of heuristic search algorithms. Front Neuroinformatics 11:6
120. Hwang HJ, Choi H, Kim JY, Chang WD, Kim DW, Kim K, Jo S, Im CH (2016) Toward more intuitive brain–computer interfacing: classification of binary covert intentions using functional near-infrared spectroscopy. J Biomed Opt 21(9):091303
121. Watanabe K, Tanaka H, Takahashi K, Niimura Y, Watanabe KY (2016) NIRS-based language learning BCI system. IEEE Sens J 16(8):2726–2734
122. Liu Y, Ayaz H (2018) Speech recognition via fNIRS based brain signals. Front Neurosci 12:695
123. Sereshkeh AR, Yousefi R, Wong AT, Chau T (2019) Online classification of imagined speech using functional near-infrared spectroscopy signals. J Neural Eng 16(1):016005
124. Abibullaev B, An J, Jin SH, Moon JI (2014) Classification of brain hemodynamic signals arising from visual action observation tasks for brain–computer interfaces: a functional near-infrared spectroscopy study. Measurement 49:320–328
125. Abibullaev B, An J, Lee SH, Moon JI (2017) Design and evaluation of action observation and motor imagery based BCIs using near-infrared spectroscopy. Measurement 98:250–261
126. Mihara M, Hattori N, Hatakenaka M, Yagura H, Kawano T, Hino T, Miyai I (2013) Near-infrared spectroscopy–mediated neurofeedback enhances efficacy of motor imagery–based training in poststroke victims a pilot study. Stroke 44(4):1091–1098
127. Lapborisuth P, Zhang X, Noah A, Hirsch J (2017) Neurofeedback-based functional near-infrared spectroscopy upregulates motor cortex activity in imagined motor tasks. Neurophotonics 4(2):021107
128. Aranyi G, Pecune F, Charles F, Pelachaud C, Cavazza M (2016) Affective interaction with a virtual character through an fNIRS brain–computer interface. Front Comput Neurosci 10:70
129. Luhrs M, Goebel R (2017) Turbo-Satori: a neurofeedback and brain–computer interface tool box for real-time functional near-infrared spectroscopy. Neurophotonics 4(4):041504
130. Batula AM, Kim YE, Ayaz H (2017) Virtual and actual humanoid robot control with four-class motor-imagery-based optical brain–computer interface. Biomed Res Int 2017:1463512
131. Wyser DG, Lambercy O, Scholkmann F, Wolf M, Gassert R (2017) Wearable and modular functional near-infrared spectroscopy instrument with multidistance measurements at four wavelengths. Neurophotonics 4(4):041413
132. Shin J, Kwon J, Choi J, Im CH (2018) Ternary near-infrared spectroscopy brain–computer interface with increased information transfer rate using prefrontal hemodynamic changes during mental arithmetic, breath-holding, and idle state. IEEE Access 6:19491–19498
133. Shin J, Kim DW, Müller KR, Hwang HJ (2018) Improvement of information transfer rates using a hybrid EEG-NIRS brain–computer interface with a short trial length: offline and pseudo-online analyses. Sensors 18(6):1827
134. Hong KS, Pham PT (2019) Control of axially moving systems: a review. Int J Control Autom Syst 17(12):2983–3008
135. Li Z, Jiang YH, Duan L, Zhu CZ (2017) A Gaussian mixture model based adaptive classifier for fNIRS brain–computer interfaces and its testing via simulation. J Neural Eng 14(4):046014
136. Zhang S, Zheng Y, Wang D, Wang L, Ma J, Zhang J, Xu W, Li D, Zhang D (2017) Application of a common spatial pattern-based algorithm for an fNIRS-based motor imagery brain–computer interface. Neurosci Lett 655:35–40
137. Kaiser V, Bauernfeind G, Kreilinger A, Kaufmann T, Kubler A, Neuper C, Muller-Putz GR (2014) Cortical effects of user training in a motor imagery based brain–computer interface measured by fNIRS and EEG. Neuroimage 85:432–444
138. Blokland Y, Spyrou L, Thijssen D, Eijsvogels T, Colier W, Floor-Westerdijk M, Vlek R, Bruhn J, Farquhar J (2014) Combined EEG-fNIRS decoding of motor attempt and imagery for brain switch control: an offline study in patients with tetraplegia. IEEE Trans Neural Syst Rehabil Eng 22:222–229
139. Putze F, Hesslinger S, Tse CY, Huang YY, Herff C, Guan CT, Schultz T (2014) Hybrid fNIRS-EEG based classification of auditory and visual perception processes. Front Neurosci 8:373
140. Morioka H, Kanemura A, Morimoto S, Yoshioka T, Oba S, Kawanabe M, Ishii S (2014) Decoding spatial attention by using cortical currents estimated from electroencephalography with near-infrared spectroscopy prior information. Neuroimage 90:128–139
141. Koo B, Lee HG, Nam Y, Kang H, Koh CS, Shin HC, Choi S (2015) A hybrid NIRS-EEG system for self-paced brain computer interface with online motor imagery. J Neurosci Methods 244:26–32
142. Yin XX, Xu BL, Jiang CH, Fu YF, Wang ZD, Li HY, Shi G (2015) A hybrid BCI based on EEG and fNIRS signals improves the performance of decoding motor imagery of both force and speed of hand clenching. J Neural Eng 12:036004
143. Lee MH, Fazli S, Mehnert J, Lee SW (2015) Subject-dependent classification for robust idle state detection using multi-modal neuroimaging and data-fusion techniques in BCI. Pattern Recognit 48:2725–2737
144. Buccino AP, Keles HO, Omurtag A (2016) Hybrid EEG-fNIRS asynchronous brain–computer interface for multiple motor tasks. PLoS ONE 11:0146610
145. Ahn S, Nguyen T, Jang H, Kim JG, Jun SC (2016) Exploring neuro-physiological correlates of drivers' mental fatigue caused by sleep deprivation using simultaneous EEG, ECG, and fNIRS data. Front Hum Neurosci 10:219
146. Li R, Potter T, Huang W, Zhang Y (2017) Enhancing performance of a hybrid EEG-FNIRS system using channel selection and early temporal features. Front Hum Neurosci 11:462
147. Aghajani H, Garbey M, Omurtag A (2017) Measuring mental workload with EEG plus fNIRS. Front Hum Neurosci 11:359
148. Liu Y, Ayaz H, Shewokis PA (2017) Mental workload classification with concurrent electroencephalography and functional near-infrared spectroscopy. Brain–Computer Interfaces 4(3):175–185
149. Shin J, Müller KR, Schmitz CH, Kim DW, Hwang HJ (2017) Evaluation of a compact hybrid brain–computer interface system. Biomed Res Int 2017:6820482
150. Omurtag A, Aghajani H, Keles HO (2017) Decoding human mental states by whole-head EEG+ FNIRS during category fluency task performance. J Neural Eng 14(6):066003

151. Zhang M, Hua Q, Jia W, Chen R, Su H, Wang B (2018) Feature extraction and classification algorithm of brain–computer interface based on human brain central nervous system. NeuroQuantology 16(5):896–900
152. Chiarelli AM, Croce P, Merla A, Zappasodi F (2018) Deep learning for hybrid EEG-fNIRS brain–computer interface: application to motor imagery classification. J Neural Eng 15(3):036028
153. Zafar A, Hong KS (2018) Neuronal activation detection using vector phase analysis with dual threshold circles: a functional near-infrared spectroscopy study. Int J Neural syst 28(10):1850031
154. Erdoğan SB, Özsarfati E, Dilek B, Kadak KS, Hanoğlu L, Akin A (2019) Classification of motor imagery and execution signals with population-level feature sets: implications for probe design in fNIRS based BCI. J Neural Eng 16:026029
155. Khan MJ, Ghafoor U, Hong KS (2018) Early detection of hemodynamic responses using EEG: a hybrid EEG-fNIRS study. Front Hum Neurosci 12:479
156. Yaqub MA, Woo SW, Hong KS (2018) Effects of HD-tDCS on resting-state functional connectivity in the prefrontal cortex: an fNIRS study. Complexity 2018:1613402
157. Ghafoor U, Lee JH, Hong KS, Park SS, Kim J, Yoo HR (2019) Effects of acupuncture therapy on MCI patients using functional near-infrared spectroscopy. Front Aging Neurosci 11:237
158. Hong KS, Yaqub MA (2019) Application of functional near-infrared spectroscopy in the health industry: a review. J Innov Opt Health Sci 12(6):1930012
159. Yang D, Hong KS, Yoo SH, Kim CS (2019) Evaluation of neural degeneration biomarkers in the prefrontal cortex for early identification of patients with mild cognitive impairment: an fNIRS study. Front Hum Neurosci 13:317
160. Bhutta MR, Hong KS, Kim BM, Hong MJ, Kim YH, Lee SH (2014) Note: three wavelengths near-infrared spectroscopy system for compensating the light absorbance by water. Rev Sci Instrum 85:026111
161. Curtin A, Ayaz H (2018) The age of neuroergonomics: towards ubiquitous and continuous measurement of brain function with fNIRS. Jpn Psychol Res 60(4):374–386
162. Yi G, Mao JX, Wang YN, Guo SY, Miao ZQ (2018) Adaptive tracking control of nonholonomic mobile manipulators using recurrent neural networks. Int J Control Autom Syst 16(3):1390–1403
163. Petrantonakis PC, Kompatsiaris I (2018) Single-trial NIRS data classification for brain–computer interfaces using graph signal processing. IEEE Trans Neural Syst Rehabil Eng 26(9):1700–1709
164. Kazemy A, Cao J (2018) Consecutive synchronization of a delayed complex dynamical network via distributed adaptive control approach. Int J Control Autom Syst 16(6):2656–2664
165. Nguyen HD, Hong KS (2016) Bundled optode implementation of 3D imaging in functional near-infrared spectroscopy. Biomed Opt Express 7(9):3419–3507